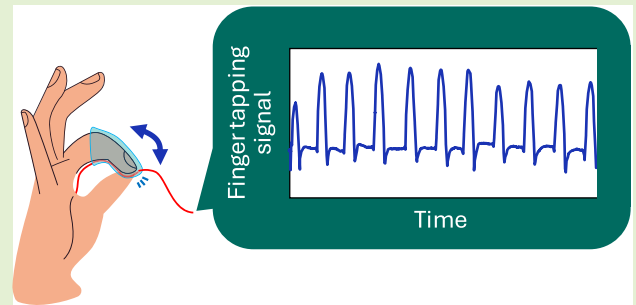


Finger Tapping Test Evaluated by Embedded Fiber Bragg Gratings

Elena De Vita¹, Member, IEEE, Vincenzo Romano Marrazzo², Giovanni Breglio¹,
Agostino Iadicicco¹, Member, IEEE, and Stefania Campopiano¹, Member, IEEE

Abstract—The finger tapping (FT) test is a widely used neuropsychological assessment designed to measure fine motor skills, like speed and coordination of finger movements, particularly used in diagnosing and tracking neurological conditions that affect motor control. Nowadays, despite the spread of this test, FT is clinically evaluated by observing the patient executing several FT tasks (FTTs) and assigning a score to the FT performance based on rating scales, depending on the specific pathology to be diagnosed. Hence, there is a need for a device that supports clinicians in evaluating the execution of the FTTs for specific patients by providing quantitative information. Therefore, this work presents a novel FT sensor based on fiber Bragg grating (FBG) and its embedding in flexible and wearable compounds. The proposed sensor consists of a fiber Bragg grating (FBG) embedded in a silicone thimble that can be easily worn during functional tests (FTs). This design is flexible, lightweight, and minimally invasive, effectively overcoming the challenges posed by other devices discussed in the literature. The developed FBG thimble has been tested on eight volunteers during three different FTTs, i.e., random, synchronized, and quick tapping (QT), performed using both hands to record and compare the FT waveforms by varying subject, hand, and kind of movement. The sensor has proved to be able to measure the tapping signals in real time and provide information about several FT parameters of clinical interest, such as force touch, rhythmicity, and motor coordination. Moreover, the spectral analysis of the recorded signals has been carried out to compare the subjects' recordings for each FTT, highlighting the differences among them in terms of movement periodicity and regularity.

Index Terms—Fiber Bragg grating (FBG), finger dexterity, Finger tapping (FT), neurodegenerative diseases diagnosis, wearable sensors.



I. INTRODUCTION

FINGER tapping (FT) test is a commonly used assessment tool to evaluate fine motor control, coordination, and speed. It involves tapping a finger, typically the index finger, usually on a surface, since the analysis of this kind of movement can be utilized in assessing motor dysfunction, bradykinesia, coordination problems, effects of treatments, and efficacy of drugs (i.e., during follow up) [1], and in tracking

disease progression [2]. More generally, FT tasks (FTTs) also include other fingers or some objects/body parts in the movement, as in the hand-to-thigh tapping or the piano-playing-like tapping (i.e., table tapping) [3]. Moreover, the kind of FTT can depend on the specific instructions to follow, e.g., index tapping as quickly as possible for a specified duration, alternate tapping between index and middle fingers of one hand as quickly as possible, tapping a sequence of fingers in a specified order as quickly as possible, tapping the fingers of one hand or the other hand depending on handedness, tapping fingers in a rhythmic pattern, and mirrored tapping to have a visual cue [4], [5], [6], [7]. Thus, the selected FTT can vary by the goals of the assessment, the tested population, and the reference testing protocol.

The FT test is used in a variety of clinical and research settings. It is particularly relevant for:

- 1) Neurological patients, such as in case of Parkinson's disease (PD), ataxia, Alzheimer's disease, essential tremor, Korsakoff syndrome, mild cognitive impairment, dementia, and motor impairments resulting from stroke or traumatic brain injury [2], [8].
- 2) Psychiatric patients, e.g., to assess psychogenic movement disorders and major depressive disorder [9], [10].

Received 28 August 2024; revised 11 October 2024; accepted 15 October 2024. Date of publication 29 October 2024; date of current version 13 December 2024. This work was supported by the European Union - Next Generation EU under the Italian National Recovery and Resilience Plan (NRRP), Mission 4, Component 2, Investment 1.3, partnership on "Telecommunications of the Future" (PE00000001 - program "RESTART") under Grand CUP E63C22002070006. The associate editor coordinating the review of this article and approving it for publication was Dr. Xuehao Hu. (Corresponding author: Stefania Campopiano.)

Elena De Vita, Agostino Iadicicco, and Stefania Campopiano are with the Department of Engineering, University of Naples "Parthenope," 80143 Naples, Italy (e-mail: elena.devita@uniparthenope.it; agostino.iadicicco@uniparthenope.it; stefania.campopiano@uniparthenope.it).

Vincenzo Romano Marrazzo and Giovanni Breglio are with the Department of Electrical Engineering and Information Technology (DIETI), University of Naples Federico II, 80125 Naples, Italy (e-mail: vincenzoromano.marrazzo@unina.it; breglio@unina.it).

Digital Object Identifier 10.1109/JSEN.2024.3485080

- 3) Occupational and functional assessment in healthy individuals to evaluate the motor function in the upper limbs and the relationship between hand preference and hand skill, and to assess the hand skill and coordination for hands-based occupations [11].

Concerning the method by which FTTs are evaluated, clinicians currently rely on the observation of the patient while executing the tasks and on rating scales. There are several rating scales that include FTTs, each one related to specific pathologies. First among all are the Unified Parkinson's Disease Rating Scale (UPDRS) and Movement Disorder Society-sponsored revision of the UPDRS (MDS-UPDRS), which in the motor section evaluates the patient's difficulties in the FTT execution with a score from 0 to 4. Indeed, according to the MDS-UPDRS, FTT can contribute to identifying bradykinesia, which is the prerequisite for PD diagnosis, by pointing out movement slowness, decrementing speed, and/or hesitations [12]. Other rating scales including FTTs are: 1) Bain and Findley Clinical Tremor Rating Scale, which involves a FTT to evaluate upper extremity postural tremor in patients with multiple sclerosis [13]; 2) nine-hole peg test (NHPT), developed to measure finger dexterity in a wide range of populations, including patients with stroke [14]; 3) Jebsen-Taylor Hand Function Test used to assess hand function and manual dexterity also in individuals with hand injuries or neurological conditions [15]; 4) abnormal involuntary movement scale (AIMS) to assess severity of dyskinesias like extremity, truncal, and orofacial movements in patients taking antipsychotic medications [16]; 5) montreal cognitive assessment (MoCA), consisting in a cognitive assessment tool which includes a section of alternating tapping that evaluates hand-eye coordination and speed by tapping with alternating index fingers [17]; and 6) halstead-reitan neuropsychological test battery, used to investigate the human abilities compromised by brain injury and including FTTs for the injuries localization [18].

Although rating scales are noninvasive and clinically widespread, they are also qualitative or at most semiquantitative, and results are affected by interrater variability and low reliability, especially for cross-diagnostic comparison [1]. For example, bradykinesia-related items have the lowest reliability among the tasks provided by UPDRS, particularly for the assessment of the FTT and when the severity is slight or mild. Practically misdiagnosis of PD is much common, and essential tremor in the early stage is easily confused with PD. Therefore, the medical community would benefit from novel objective, inexpensive, and simple methods and devices able to accurately monitor the FT test by recording several parameters related to FT performance, like tapping speed and rhythm, inter-tap interval, the distance between fingers, the force of the tap, symmetry and kinematics of the movements [19]. For this reason, several measurement systems and devices have been proposed in the literature to record FTTs. They can be classified into four main categories: 1) 3-D motion capture systems; 2) touch pad-like sensors; 3) finger-mounted sensors; and 4) hybrid sensors, which include sensing elements belonging to motion capture systems and inertial sensors of finger-mounted devices.

Three-dimensional motion capture systems rely on motion analysis to extract and evaluate the movement of the fingers and include motion capture camera systems and markers [20], 3-D depth sensors [21], and computer vision-based systems [22]. Among their advantages, passivity and non-invasiveness stand out. Moreover, they can be integrated with virtual environments to provide and analyze different tasks [23]. However, these systems are commonly optimized primarily for whole-body detection, exhibiting poor spatial accuracy for detecting smaller movements like FT. In addition, the use of several cameras involves the need for a large laboratory and high costs. Moreover, camera markers can be obstructed while patients are performing FTTs and measurement accuracy varies depending on the environmental interferences like lighting conditions and reflective surfaces, and on the patient's characteristics like size and shape of the fingers.

Touch pads-like sensors include digitomography pads [1], [24], [25], keyboards [26], at-home testing equipment [27], smartphones [28], and tablets [29], and usually evaluate FT on a pad instead of the opposition movement between fingers. This kind of FT sensor offers intuitive patient-device interaction, versatile use, multi-touch support, compactness, and portability. On the other hand, they typically have a fixed grid of sensing elements, which can limit the spatial resolution of the measurement. In addition, they lack detailed kinematic information since they capture contact or pressure information rather than finger trajectories, velocities, or accelerations. Moreover, these pads can be also influenced by external factors like moisture and dirt which can affect the touchpad sensitivity, responsiveness, or detection accuracy, potentially introducing errors or artifacts into the FT analysis.

Finger-mounted sensors are more or less miniaturized devices directly applied to one or more fingers (and sometimes also on the wrist), being based on accelerometer and gyroscopes [12], [30], magnetic sensors [31], [32], touch and force sensors [19], [33], and infrared emitting diodes [34]. Their benefits with respect to the previously reported kinds of FT sensors consist of more precise and accurate tapping detection, individual finger monitoring, real-time feedback, and comprehensive data capture. At the same time, these sensors can affect the patient's movements and influence the results because of their weight, their unnatural form, and the connected wires, which can be distracting. Moreover, their components can be sensitive to environmental factors like temperature, humidity, or electrical interference. In addition, devices like accelerometers require special calibration procedures, and magnetic sensors are prone to artifacts when the mutual orientation of coils is changed.

Finally, hybrid sensors combine the advantages of sensors belonging to different categories and integrate a reference sensor. This is the case of [35], where two gyroscopes are mounted on the thumb and index finger and connected to their control units, a force transducer is mounted on the index fingertip and these sensors are combined with six markers to compare the measured results with respect to the motion capture camera outcomes. However, it is worth noting that hybrid sensors are complex systems since they introduce high

costs and challenges of synchronization between the multiple sensing technologies which may introduce crosstalk or interference. Furthermore, data fusion complexity can require sophisticated algorithms and processing techniques to integrate the data.

In this scenario, this work proposes a novel FT sensor. It is built upon fiber optic technology, in particular fiber Bragg grating (FBG), and its embedding in silicone compound to obtain a stretchable and wearable sensor. Integrating FBG sensors into various materials not only expands their range of applications, making them particularly suitable for monitoring and diagnostics but also enhances their wearability, user comfort, and the practicality of the final device [36]. Among the variety of materials under investigation to improve FBG sensitivity and feasibility for different medical purposes, polymeric matrices like silicone are increasingly gaining attention due to their flexibility and ease of integration. In recent years, silicone-embedded FBGs have been used in monitoring various vital physiological signals and activities such as body temperature, heart rate, and breathing, for cardiorespiratory and biomechanical analysis, to sensorize endoscopes, catheters, surgical tools, and more [37].

In this framework, this work presents an FBG-based FT sensor showing a finger glove shape so that it can be easily worn while performing the FTTs. Therefore, the proposed solution is a sensorized thimble, falling into the finger-mounted category of sensors but embedding an FBG as a sensitive element and thus exhibiting extremely lightweight (i.e., minimally invasiveness), immunity to external interferences, and flexibility unlike the devices previously proposed in the literature. With respect to the previously developed sensors based on FBG encapsulation in soft materials, herein for the first time the FBG embedding strategy is aimed at monitoring FT movements. Unlike traditional embedded FBG sensors, which are typically integrated into fabric wristbands, belts, or clothes, this work reports on a silicone FBG-equipped thimble designed to be inherently wearable, allowing for seamless integration, enhanced comfort during use, easy manufacture and maintenance, and high adaptability and customizability depending on the type of involved silicone, thimble thickness, and its geometry, all features that can affect the levels of sensitivity and allow the sensor to respond to different ranges of motion. In the following, the steps implemented toward the development of such a new FT sensor, i.e., its design, fabrication, and testing during FTTs, are reported, and results are discussed.

II. SENSOR FABRICATION AND CONCEPT

In this Section, the steps that have led to the development of the proposed FT sensor and its working concept are described.

A. Operating Principle of FBGs

First, as mentioned in the Introduction, the sensor consists of a soft thimble whose sensing component is an FBG embedded inside. An FBG is a fiber optic sensor obtained by periodically modifying the refractive index (RI) of the optical fiber core. Such an RI perturbation is able to reflect a narrow portion

of the wavelength of the input light acting as a band-reject filter [38]. The reflected spectrum is centered around the Bragg wavelength, denoted by λ_B , which is equal to the double product of the effective RI of the guided core mode, i.e., n_{eff} , multiplied by the spatial period of the FBG, i.e., Λ , as reported in the following equation [38], [39]:

$$\lambda_B = 2n_{\text{eff}}\Lambda. \quad (1)$$

Since variations in the environmental parameters like strain and temperature affect both n_{eff} and Λ , these physical magnitudes induce perturbations of the FBG spectral properties which are commonly used for sensing applications. Indeed, in correspondence of strain and/or temperature changes around the FBG, a shift of the Bragg wavelength, i.e., $\Delta\lambda_B$, can be observed from the spectrum, as reported in the following equation:

$$\Delta\lambda_B = \lambda_B \left\{ 1 - \frac{n^2}{2} [p_{12} - \nu(p_{11} + p_{12})] \right\} \varepsilon + \lambda_B (\alpha + \xi) \Delta T. \quad (2)$$

The first term of the external sum in (2) is the Bragg wavelength shift due to the strain effect, whereas the second term is the shift due to the temperature variation effect. In particular, for the strain term, the following parameters occur: the components of the strain-optic tensor are p_{11} and p_{12} ; the RI of the core is denoted by n ; the Poisson's ratio is ν ; and the axial strain is ε . For the temperature variation term, instead, α denotes the thermal expansion coefficient of the fiber material (usually silica), ξ indicates the thermo-optic coefficient, and ΔT is the temperature change [38].

This relationship between λ_B shift and environmental parameters enables the sensing of strain, temperature, or potentially other measurands like load, pressure, vibrations, and so on. For the application proposed in this work, the FBG is needed to perform pressure measurements, and thus to sense the strain variations induced by the pressure exerted by the finger on the FBG during the tapping, as shown in the following paragraph. In isotropic materials, indeed, the stress induced by the applied pressure can be related to strain using Hooke's law, i.e., by means of the proportionality coefficient represented by the material Young's modulus. Therefore, to obtain the strain-induced λ_B shift, the ΔT contribution is neglected and (2) becomes

$$\frac{\Delta\lambda_B}{\lambda_B} = S\varepsilon \quad (3)$$

where the strain sensitivity S is typically $1.2 \text{ pm}/\mu\varepsilon$ for a bare FBG. In our case, the involved FBG is 5 mm long and bare before the process of embedding into the silicone matrix, as reported in the following.

B. FT Sensor Concept and Fabrication

The basis for the proposed FT sensor lies in the combination of 3-D printing with FBG embedment, as schematically described in Fig. 1. FBG embedment technique in silicone rubber has been proved to provide flexible packaging able to make the FBG sensitive to the applied external pressure while insulating it from longitudinal strain perturbations [40].

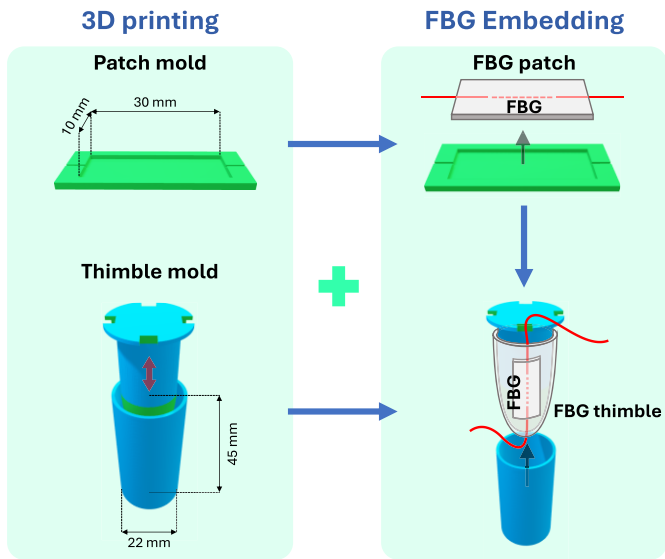


Fig. 1. Schematic representing the combination of 3-D printing and embedding strategies for obtaining the FBG thimble for FT sensing.

The sensing mechanism, indeed, is based on the expansion of the silicone rubber which embeds the FBG in the plane orthogonal to the direction of compression. In other words, if the FBG is embedded within a silicone patch, when the finger exerts pressure on the latter during the first part of tapping, the silicone rubber extends causing the FBG strain (i.e., stretching) along its direction. Subsequently, when the finger moves away from the silicone patch during the last part of tapping, the FBG returns to its starting length, experiencing a strain (i.e., compression). Therefore, silicone embedding is involved as a key strategy to sense the finger pressure exerted on the FBG during the performed FTT, so that by measuring the strain variations of the FBG through (3) an indirect measure of the FT pressure can be obtained. On the other hand, 3-D printing is a precursor to the embedding of the FBG since it provides customizable molds allowing to shape the silicone matrix, initially in liquid form, based on the application. In particular, 3-D printing through fused deposition technique is employed for fabricating PLA molds for silicone patches and thimble aiming to shape the silicone sensor.

To report the fabrication process step by step, the patch mold allows to obtain a silicone patch embedding a bare and 5 mm long FBG, placed in the middle of the patch. The involved silicone material is Dragon Skin 10 Medium, which exhibits skin compatibility, a wide range of operating temperatures, and ease of use during the fabrication steps like a mixture of the components, pouring, and curing. The patch is fabricated by following the procedure described in [40], and its dimensions are $30 \times 10 \times 1.3$ mm. It exhibits a temperature sensitivity of $10.5 \text{ pm}/^\circ\text{C}$, close to the bare FBG one; a low strain sensitivity of $5.9 \cdot 10^{-2} \text{ pm}/\mu\epsilon$, and a sensitivity to forces applied perpendicularly to the embedded FBG of $9.2 \text{ pm}/\text{N}$ [40], [41], [42], [43].

Once fabricated the patch embeds the FBG and the patch itself is embedded in a silicone thimble made of the same

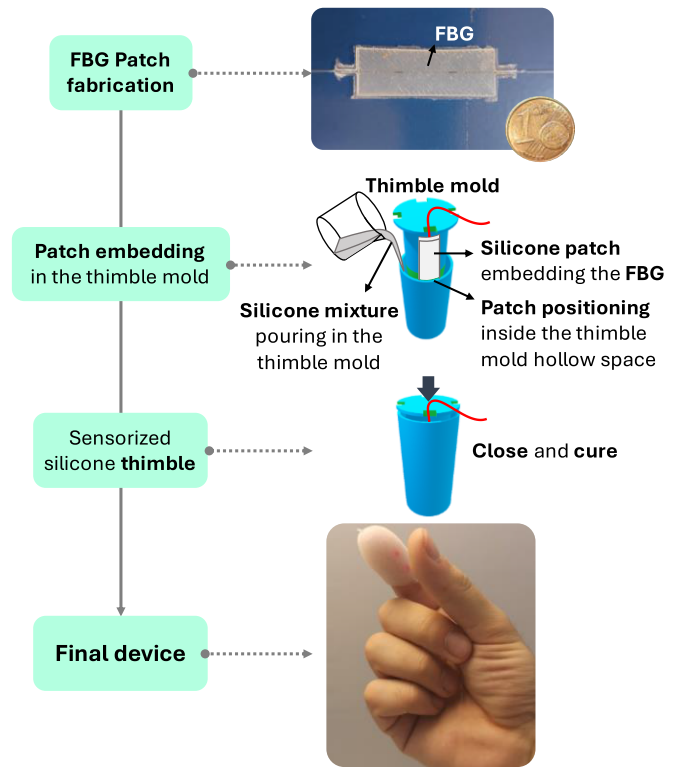


Fig. 2. Steps of fabrication of the FBG thimble from the patch to its embedding in the silicone thimble to obtain the final device.

kind of silicone by following the steps reported in Fig. 2. For obtaining the thimble, a new mold is printed, made of two components, i.e., a cylindrical base with a cavity showing a fingertip shape, and a fingertip shaped cover (as already shown in Fig. 1). Then, the previously developed patch embedding the FBG is placed inside the gap between base and cover of the thimble mold. It is worth noting that there is a small hole at the center of the mold base that allows one fiber end to come out from the mold, whereas the other end can pass through one of the grooves of the mold cover. Finally, by pouring the silicone mixture into the gap between the two components of the thimble mold, after waiting for the curing time, it is possible to extract the final device, i.e., the silicone thimble embedding the patch, and thus the FBG, ready for FT sensing.

C. Sensor Readout

Since the FBG sensor working principle is based on wavelength encoding, when it undergoes pressure variations a wavelength shift is produced. From what just said, by monitoring the FBG spectrum, the latter will move forward or backward if a stretch or a compression is applied, respectively.

An experimental demonstration is depicted in Fig. 3, in which the fabricated sensor worn on the index finger is shown with its relative reflected spectrum. It is worth noting that when the structure is at rest (Fig. 3(a), left) the FBG spectrum is constant and centered around a specific λ_B (Fig. 3(a), right). When a pressure is applied (i.e., performing a tapping as shown in Fig. 3(b), left), the FBG spectrum moves through the shifting of its λ_B (Fig. 3(b), right).

For the case study here proposed, different kinds of FTTs are performed and monitored by tapping the index finger and

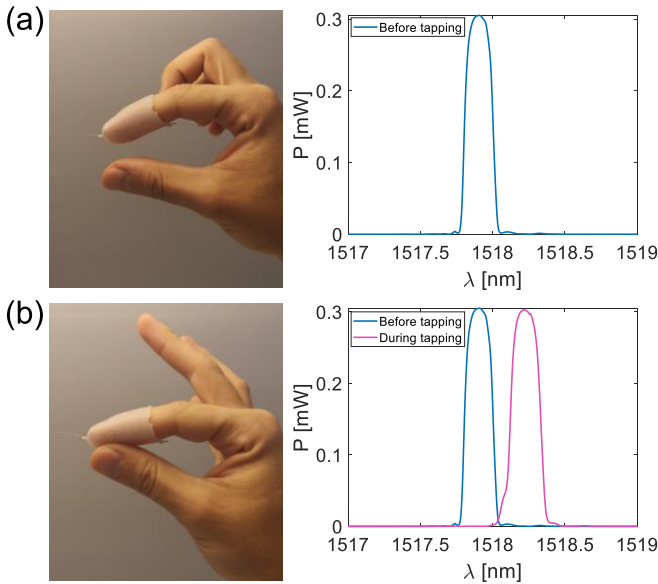


Fig. 3. Working principle of FBG thimble for FT sensing (a) on the left, photograph of the worn sensor before tapping the index finger on the thumb, and on the right, spectrum of the FBG embedded inside the thimble and (b) on the left, photograph of the sensor during the tapping, and on the right, shifted spectrum of the embedded FBG due to the tapping.

wearing the FBG thimble with the thumb using the right- (RH) or left-hand (LH). Particularly, the FTTs acquired from the sensor are:

- 1) random tapping (RT), by tapping randomly;
- 2) synchronized tapping (ST), i.e., FT in cue-priming condition, by tapping periodically using a metronome set at 120 beats per minute (bpm) as an audio cue;
- 3) quick tapping (QT), by tapping as fast as possible.

Each FTT is achieved by different subjects in the same time interval. The sensor output is monitored by means of a dedicated optoelectronic system (i.e., interrogator), elaborating the input optical signal related to the FBG central wavelength into digital data. The employed instrument is the micrometer optics interrogator (MOI) sm130, based on the tunable laser technology, making it one of the most performant systems in terms of accuracy and resolution, with the further task of acquiring the whole FBG sensor spectrum. Moreover, it shows a bandwidth of 2 kHz, which can be decreased with data interleaving, allowing to have a pre-filtered signal during the acquisition. The experimental setup is depicted in Fig. 4.

Data from the interrogator are sent to a PC through an ethernet connection. Dedicated software allows for monitoring of the FBG central wavelength response and acquiring data in a log file. For this case study, data are further processed in a MATLAB environment with in-time and in-frequency analyses.

III. EXPERIMENTAL RESULTS AND DISCUSSION

In this Section, experimental tests of the FBG thimble measurements are reported. Results are shown for different tasks, performed with both hands. Moreover, different subjects have been assessed to show that the proposed solution is able to detect the dependence of the FT outcomes on these multiple factors. The results are in terms of trends of λ_B

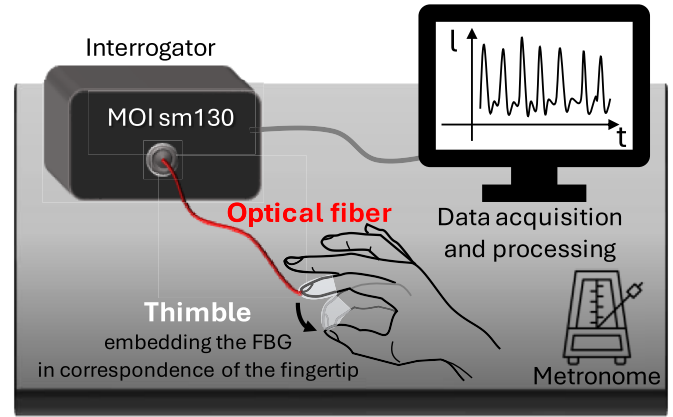


Fig. 4. Experimental setup schematic: the FBG thimble is connected to the interrogator through the FBG optical fiber enabling the interrogator to measure the wavelength encoded tapping data. FBG-related data are then acquired and processed from the interrogator with a PC.

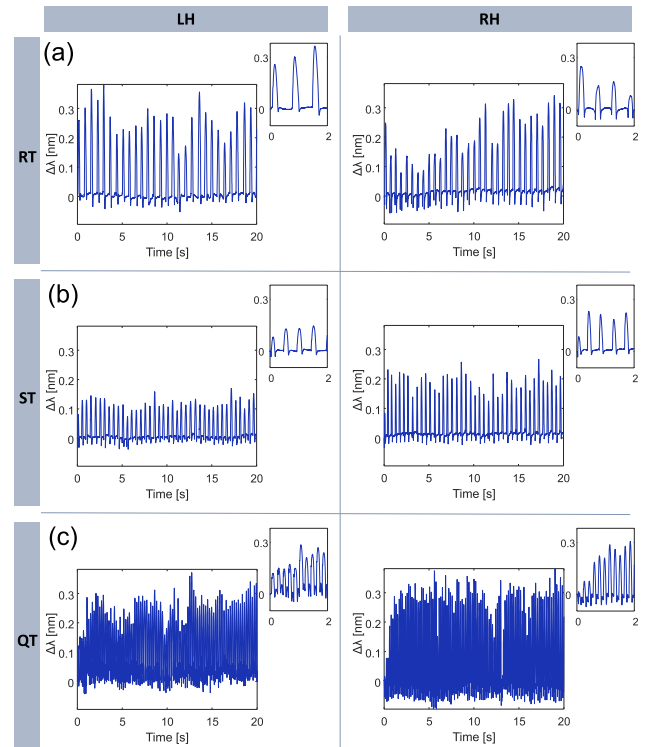


Fig. 5. FBG thimble recordings for three kinds of FTTs performed by the same subject. (a) RT. (b) ST. (c) QT. Results reported in the left column correspond to the signals recorded with the LH, whereas results in the right column correspond to the RH signals. For each plot, a zoomed-in view correspondence of the first 2 s of recording is reported at the top right to highlight the shape of the tapping waveforms for the correspondent subject and task.

shift (i.e., $\Delta\lambda_B$) as a function of the time, recorded by the FBG thimble and collected by the optical interrogator during each FTT.

A. Comparison Among Different FTTs

The FBG thimble recordings during three FTTs, i.e., RT, ST, QT, performed by the same subject using one time the LH and the second time the RH, are reported in Fig. 5. For the sake of clarity, a time frame of 20 s is shown for each temporal plot. The first and second columns correspond to the results obtained for the LH and the RH

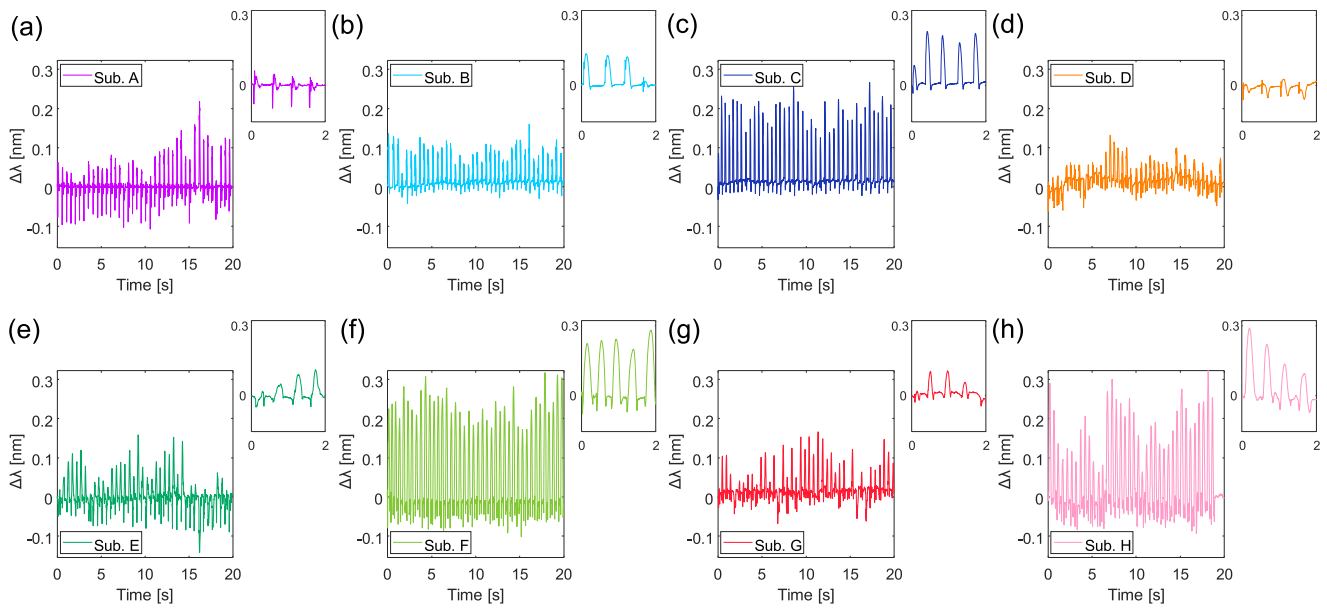


Fig. 6. FBG thimble recordings for different subjects [from (a) to (h)] performing the ST task with RH following the metronome set at 120 bpm. For each plot, a zoomed-in view correspondence of the first 2 s of recording is reported at the top right to highlight the shape of the tapping waveforms for the correspondent subject.

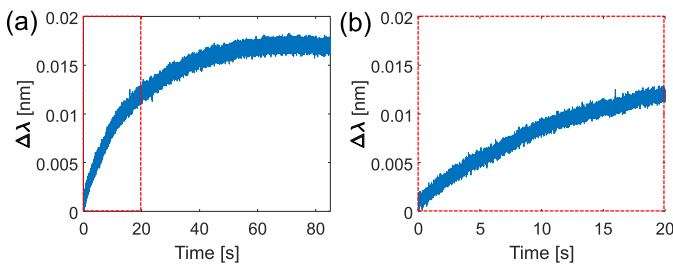


Fig. 7. (a) FBG thimble recording for a volunteer wearing the FBG thimble for about 85 s without performing any FFT. (b) Zoom on the first 20 s showing the increasing trend of $\Delta\lambda$ due to the higher temperature of the finger with respect to the thimble.

performing the tapping, respectively, whereas the rows correspond to the kind of executed task.

As shown in Fig. 5, the measured trends show a sequence of peaks, each one corresponding to the tapping exerted by the index finger (i.e., the finger wearing the thimble) on the thumb, where the amplitude of the peaks depends on the extent of applied pressure and can vary according to the kind of performed task and the involved hand. Therefore, the peaks correspond to the tapping waveforms. For each Fig. 5, a temporal zoomed-in view of a range of $0 \div 2$ s is reported at the top right of the full plot to better show the tapping waveform. The zoomed profiles can be useful, especially for the QT recordings, where the peaks are very close to each other since the subject's tapping is performed as fast as possible.

In the case of ST, about 40 peaks in 20 s can be observed (i.e., 40 peaks for the LH and 41 for the RH) since the metronome was set at 120 bpm, denoting the subject's capability to hold the pace of the audio cue and the variability between the hands executing the task.

B. Comparison Among Different Subjects

The FBG thimble has been tested on different subjects. Therefore, Fig. 6 reports the recordings of ST, still performed with a metronome at 120 bpm as an audio cue, for 8 volunteers

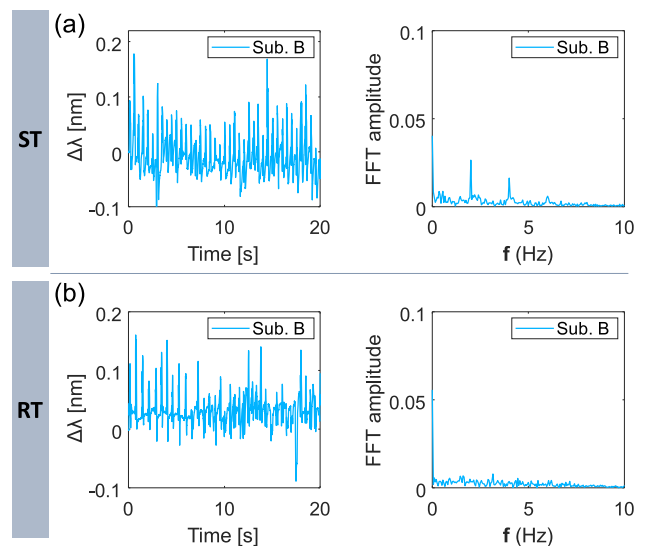


Fig. 8. FBG thimble recordings (left column) and the corresponding FFT (right column) for the same subject (i.e., Sub. B) performing ST (a) and RT (b) with the RH.

denoted by the letters from A to H and different line colors. Also in this case, the waveform of the recorded peaks is highlighted in the temporal zoom reported at the top right for each full plot of 20 s.

It is worth noting, especially by observing the zoomed plots, that the shape of the tapping waveform varies according to the subject performing the task. Indeed, many features of the tapping waveform, such as peak amplitude, shape regularity, and the presence of negative peaks before and/or after each tapping peak, are almost repeatable for the same subject but can vary among different subjects. For example, for the first and fourth volunteers, i.e., Sub. A and D (Fig. 6(a) and (d), respectively), the tapping waveform is characterized by a lower peak amplitude preceded by a larger negative peak, features which are missing in the other subjects. The presence of a negative pre-peak could be due to a slight thimble deformation

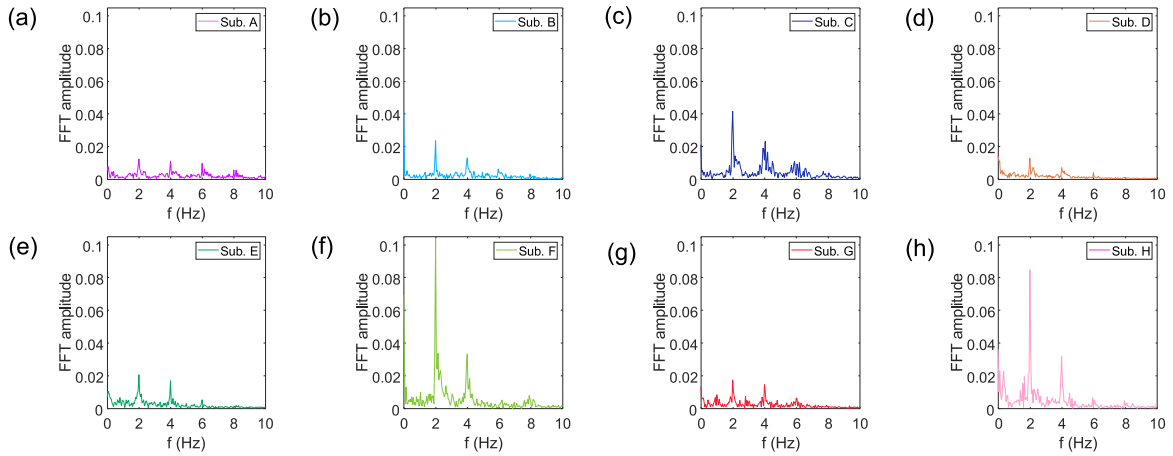


Fig. 9. FFT of the signals recorded for each subject of Fig. 6 [from (a) to (h)] performing ST task with RH following the metronome set at 120 bpm.

caused by a light starting pressure exerted by the index finger from inside the thimble on the embedded FBG right before the index–thumb touch. On the contrary, the negative post-peak could be due to the sudden thimble decompression caused by the quick finger release, or to the non-linear elastic response of the silicone during its shape recovery. In addition, by observing the waveforms of Sub. E [Fig. 6(e)], for example, some asymmetries between the upward and downward profiles of the tapping peak can be found, denoting different speeds of closing and opening movements of the fingers during the tapping.

Moreover, in some cases tapping waveforms appear more irregular, i.e., for Sub. D and E [Fig. 6(d) and (e)]. Furthermore, the baseline trend of the FBG thimble recording can vary among the subjects due to its sensitivity to the temperature variations of the finger skin in contact with the thimble (e.g., Sub. D and H, Fig. 6(d) and (h), respectively). However, the fluctuations of the baseline follow slow dynamics completely different from the tapping signals, so that they can be easily distinguished and filtered. Fig. 7(a) shows the recording of a volunteer wearing the FBG thimble for about 85 s without performing any FTT to better show the temperature contribution to the baseline trend. In Fig. 7(b), a zoom on the first 20 s is shown highlighting the increasing $\Delta\lambda$ trend due to the finger temperature which is slightly higher than the thimble one. After about 50 s, a plateau can be observed, denoting that the finger temperature is about 1.7 °C higher than the thimble one.

C. Comparison Among the FFT

A frequency analysis of the recorded FT signals has been performed by calculating the fast Fourier transform (FFT) for each measured trend aiming to evaluate the differences among different tasks and subjects.

Fig. 8 shows on the left the temporal signal recorded when Sub. B performs ST [Fig. 8(a)] and RT [Fig. 8(b)], and on the right the corresponding FFT. In contrast to RT, in the spectral analysis, the periodicity of the ST recording results in a peak at 2 Hz, which corresponds to the frequency of 120 bpm set at the metronome, i.e., the execution frequency of the task.

To quantify the subjects' rhythmicity in executing the ST task and to highlight the differences among them, the FFT has also been calculated for each signal in Fig. 6 and reported

in Fig. 9 correspondingly. As expected, a significant peak at 2 Hz, corresponding to the audio cue frequency, can be observed for each volunteer. In particular, Sub. C, F, and H exhibit a higher peak with respect to the other volunteers at the frequency of interest, i.e., 2 Hz, resulting in more ability to follow the pace of the metronome.

IV. CONCLUSION

FT test is performed in the clinical practice for assessing motor function and coordination in a variety of patients, from neurological ones like those suffering from Parkinson's disease to psychiatric patients. Moreover, such a test can also help in the case of occupational and functional assessment in healthy subjects.

Currently, the FT assessment is based on the clinicians' observation based on rating scales, resulting in qualitative and subjective evaluations, thus leading to low reliable diagnoses. The state-of-the-art proposes sensors that usually rely on motion capture camera systems, keyboards and tablets, accelerometers and gyroscopes, or a combination of more of these elements. However, they introduce several drawbacks, e.g., poor spatial accuracy and the need for large laboratories when cameras and markers are used, limited spatial resolution and environmental interferences in case of touchpad-like systems, bulk and subsequent artifacts for the finger-mounted devices based on inertial sensors, and data integration complexity when using hybrid structures.

Aiming to overcome such challenges, this work presents a novel FT sensor based on the embedding of an FBG in a silicone thimble, which rather than being finger-mounted can be easily worn. The silicone embedment, indeed, provides both flexibility and pressure sensitivity to the FBG sensor, resulting in a wearable, lightweight, and electrically safe FT sensor.

FBG thimble testing is carried out on eight volunteers while performing three different index-thumb FTTs, i.e., random, synchronized, and QT, each of them with both hands alternately. The FBG thimble recordings are in terms of $\Delta\lambda_B$ variations as a function of the time during 20 s of FT execution for each task, showing a trend characterized by a sequence of peaks, each one corresponding to a tapping movement, i.e., the touch between index finger, wearing the thimble, and thumb.

Such trends provide several useful information for the FT analysis. For example, the intensity of the tapping peaks is related to the pressure exerted by the subject under test,

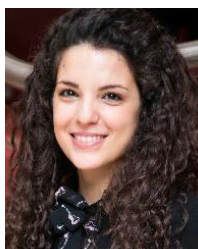
and thus it can provide information about muscle strength variations. In addition, tapping speed can be extracted from the thimble recordings obtaining insights on the dexterity of the fingers. Moreover, the tapping waveform results are specific and repeatable for each patient and simultaneously show different features among the subjects, such as the presence of negative peaks before and/or after the tapping peak of the waveform and irregularities in the upward and downward profiles of the tapping peaks. Furthermore, the spectral analysis of the recorded signals has been performed, highlighting the differences among the volunteers in terms of movement periodicity and regularity, valuable insight from the clinical perspective since periodicity can point out finger precision and motor coordination while movement irregularities may indicate muscle fatigue and grip force decrease.

In conclusion, the developed FT sensor proves to be able to monitor different FTTs in real-time without adding significant invasiveness to the procedure thanks to its flexibility and wearability. Moreover, it provides quantitative information about the dexterity of the fingers and allows for comparison of different subjects performing the tasks. Future advancements will address the customization of the FBG thimble to fit different finger sizes and will deal with the possibility of embedding more than one FBG aiming to increase the number of detectable FT parameters, including for example the distance between the tapping fingers.

REFERENCES

- [1] W. Maetzler, M. Ellerbrock, T. Heger, C. Sass, D. Berg, and R. Reilmann, "Digitomotography in Parkinson's disease: A cross-sectional and longitudinal study," *PLoS ONE*, vol. 10, no. 4, Apr. 2015, Art. no. e0123914, doi: [10.1371/journal.pone.0123914](https://doi.org/10.1371/journal.pone.0123914).
- [2] S. Suzumura et al., "Finger tapping test for assessing the risk of mild cognitive impairment," *Hong Kong J. Occupat. Therapy*, vol. 35, no. 2, pp. 137–145, Dec. 2022, doi: [10.1177/15691861221109872](https://doi.org/10.1177/15691861221109872).
- [3] A. Jobbágy, P. Harcos, R. Karoly, and G. Fazekas, "Analysis of finger-tapping movement," *J. Neurosci. Methods*, vol. 141, no. 1, pp. 29–39, Jan. 2005, doi: [10.1016/j.jneumeth.2004.05.009](https://doi.org/10.1016/j.jneumeth.2004.05.009).
- [4] D. Austin, J. McNames, K. Klein, H. Jimison, and M. Pavel, "A statistical characterization of the finger tapping test: Modeling, estimation, and applications," *IEEE J. Biomed. Health Informat.*, vol. 19, no. 2, pp. 501–507, Mar. 2015, doi: [10.1109/JBHI.2014.2384911](https://doi.org/10.1109/JBHI.2014.2384911).
- [5] S.-I. Tokushige et al., "Roles of the cerebellum and basal ganglia in temporal integration: Insights from a synchronized tapping task," *Clin. Neurophysiol.*, vol. 158, pp. 1–15, Feb. 2024, doi: [10.1016/j.clinph.2023.11.018](https://doi.org/10.1016/j.clinph.2023.11.018).
- [6] W. Kirsch and W. Kunde, "Impact of hand orientation on bimanual finger coordination in an eight-finger tapping task," *Hum. Movement Sci.*, vol. 31, no. 6, pp. 1399–1408, Dec. 2012, doi: [10.1016/j.humov.2012.02.015](https://doi.org/10.1016/j.humov.2012.02.015).
- [7] S. T. Witt, A. R. Laird, and M. E. Meyerand, "Functional neuroimaging correlates of finger-tapping task variations: An ALE meta-analysis," *NeuroImage*, vol. 42, no. 1, pp. 343–356, Aug. 2008, doi: [10.1016/j.neuroimage.2008.04.025](https://doi.org/10.1016/j.neuroimage.2008.04.025).
- [8] C. Barut, E. Kızıltan, E. Gelir, and F. Kıkırtık, "Advanced analysis of finger-tapping performance: A preliminary study," *Balkan Med. J.*, vol. 30, no. 2, pp. 71–167, Jun. 2013, doi: [10.5152/balkanmedj.2012.105](https://doi.org/10.5152/balkanmedj.2012.105).
- [9] S. Criswell, C. Sterling, L. Swisher, B. Evanoff, and B. A. Racette, "Sensitivity and specificity of the finger tapping task for the detection of psychogenic movement disorders," *Parkinsonism Rel. Disorders*, vol. 16, no. 3, pp. 197–201, Mar. 2010, doi: [10.1016/j.parkreldis.2009.11.007](https://doi.org/10.1016/j.parkreldis.2009.11.007).
- [10] X. Ma et al., "Characteristics of psychomotor retardation distinguishes patients with depression using multichannel near-infrared spectroscopy and finger tapping task," *J. Affect. Disorders*, vol. 318, pp. 255–262, Dec. 2022, doi: [10.1016/j.jad.2022.09.002](https://doi.org/10.1016/j.jad.2022.09.002).
- [11] J. E. Myers et al., "The nervous system effects of occupational exposure on workers in a South African manganese smelter," *Neurotoxicology*, vol. 24, no. 6, pp. 885–894, Dec. 2003, doi: [10.1016/s0161-813x\(03\)00081-0](https://doi.org/10.1016/s0161-813x(03)00081-0).
- [12] J. Stamatakis et al., "Finger tapping clinimetric score prediction in Parkinson's disease using low-cost accelerometers," *Comput. Intell. Neurosci.*, vol. 2013, pp. 1–13, Aug. 2013, doi: [10.1155/2013/717853](https://doi.org/10.1155/2013/717853).
- [13] R. Elble et al., "Task force report: Scales for screening and evaluating tremor: Critique and recommendations," *Mov. Disord.*, vol. 28, no. 13, pp. 1793–1800, 2013, doi: [10.1002/mds.25648](https://doi.org/10.1002/mds.25648).
- [14] K. O. Grice, K. A. Vogel, V. Le, A. Mitchell, S. Muniz, and M. A. Vollmer, "Adult norms for a commercially available nine hole peg test for finger dexterity," *Amer. J. Occupational Therapy*, vol. 57, no. 5, pp. 570–573, Sep. 2003, doi: [10.5014/AJOT.57.5.570](https://doi.org/10.5014/AJOT.57.5.570).
- [15] M. K. N. Takla, E. A. K. Mahmoud, and N. A. El-Latif, "Jebsen Taylor hand function test: Gender, dominance, and age differences in healthy Egyptian population," *Bull. Fac. Phys. Therapy*, vol. 23, no. 2, pp. 85–93, Dec. 2018, doi: [10.4103/bfpt.bfpt_11_18](https://doi.org/10.4103/bfpt.bfpt_11_18).
- [16] M. R. Munetz and S. Benjamin, "How to examine patients using the abnormal involuntary movement scale," *Psychiatric Services*, vol. 39, no. 11, pp. 1172–1177, Nov. 1988, doi: [10.1176/ps.39.11.1172](https://doi.org/10.1176/ps.39.11.1172).
- [17] J. H. Kang, Y. H. Kim, and Y.-A. Choi, "Montreal cognitive assessment and frontal assessment battery test as a predictor of performance of unaffected hand function after subcortical stroke," *Int. J. Rehabil. Res.*, vol. 44, no. 1, pp. 45–50, Mar. 2021, doi: [10.1097/mrr.0000000000000445](https://doi.org/10.1097/mrr.0000000000000445).
- [18] A. M. Horton, "Ralph M. Reitan and the clinical interpretation of neuropsychological test data," in *Evaluation and Treatment of Neuropsychologically Compromised Children*. Amsterdam, The Netherlands: Elsevier, 2020, pp. 93–106, doi: [10.1016/B978-0-12-819545-1.00005-9](https://doi.org/10.1016/B978-0-12-819545-1.00005-9).
- [19] M. Yokoe, R. Okuno, T. Hamasaki, Y. Kurachi, K. Akazawa, and S. Sakoda, "Opening velocity, a novel parameter, for finger tapping test in patients with Parkinson's disease," *Parkinsonism Rel. Disorders*, vol. 15, no. 6, pp. 440–444, Jul. 2009, doi: [10.1016/j.parkreldis.2008.11.003](https://doi.org/10.1016/j.parkreldis.2008.11.003).
- [20] R. Krupicka, Z. Szabo, S. Viteckova, and E. Ruzicka, "Motion capture system for finger movement measurement in Parkinson disease," *Radio-engineering*, vol. 23, no. 2, pp. 659–664, 2014.
- [21] B. Dror et al., "Automatic assessment of Parkinson's disease from natural hands movements using 3D depth sensor," in *Proc. IEEE 28th Conv. Electr. Electron. Engineers Isr. (IEEEI)*, Dec. 2014, pp. 1–5, doi: [10.1109/EEEI.2014.7005763](https://doi.org/10.1109/EEEI.2014.7005763).
- [22] T. Khan, D. Nyholm, J. Westin, and M. Dougherty, "A computer vision framework for finger-tapping evaluation in Parkinson's disease," *Artif. Intell. Med.*, vol. 60, no. 1, pp. 27–40, Jan. 2014, doi: [10.1016/j.artmed.2013.11.004](https://doi.org/10.1016/j.artmed.2013.11.004).
- [23] B. Galna, G. Barry, D. Jackson, D. Mhiripiri, P. Olivier, and L. Rochester, "Accuracy of the Microsoft kinect sensor for measuring movement in people with Parkinson's disease," *Gait Posture*, vol. 39, no. 4, pp. 1062–1068, Apr. 2014, doi: [10.1016/j.gaitpost.2014.01.008](https://doi.org/10.1016/j.gaitpost.2014.01.008).
- [24] S. Papapetropoulos, H. L. Katzen, B. K. Scanlon, A. Guevara, C. Singer, and B. E. Levin, "Objective quantification of neuromotor symptoms in Parkinson's disease: Implementation of a portable, computerized measurement tool," *Parkinson's Disease*, vol. 2010, pp. 1–6, Aug. 2010, doi: [10.4061/2010/760196](https://doi.org/10.4061/2010/760196).
- [25] D. R. Roalf et al., "Quantitative assessment of finger tapping characteristics in mild cognitive impairment, Alzheimer's disease, and Parkinson's disease," *J. Neurol.*, vol. 265, no. 6, pp. 1365–1375, Jun. 2018, doi: [10.1007/s00415-018-8841-8](https://doi.org/10.1007/s00415-018-8841-8).
- [26] A. J. Noyce et al., "Bradykinesia-akinesia incoordination test: Validating an online keyboard test of upper limb function," *PLoS ONE*, vol. 9, no. 4, Apr. 2014, Art. no. e96260, doi: [10.1371/journal.pone.0096260](https://doi.org/10.1371/journal.pone.0096260).
- [27] C. G. Goetz et al., "Testing objective measures of motor impairment in early Parkinson's disease: Feasibility study of an at-home testing device," *Movement Disorders*, vol. 24, no. 4, pp. 551–556, Mar. 2009, doi: [10.1002/mds.22379](https://doi.org/10.1002/mds.22379).
- [28] B. P. Printy et al., "Smartphone application for classification of motor impairment severity in Parkinson's disease," in *Proc. 36th Annu. Int. Conf. IEEE Eng. Med. Biol. Soc.*, Aug. 2014, pp. 2686–2689, doi: [10.1109/EMBC.2014.6944176](https://doi.org/10.1109/EMBC.2014.6944176).
- [29] R. Graca, R. S. Castro, and J. Cevada, "ParkDetect: Early diagnosing Parkinson's disease," in *Proc. IEEE Int. Symp. Med. Meas. Appl. (MeMeA)*, Jun. 2014, pp. 1–6, doi: [10.1109/MeMeA.2014.6860027](https://doi.org/10.1109/MeMeA.2014.6860027).
- [30] E. Rovini, D. Esposito, C. Maremmanni, P. Bongioanni, and F. Cavallo, "Using wearable sensor systems for objective assessment of parkinson's disease," in *Proc. 20th IMEKO TC4 Symp. Meas. Electr. Quantities, Res. Electr. Electron. Meas. Econ. Upturn, Together 18th TC4 Int. Workshop ADC DCA Model. Test. (IWADC)*, 2014, pp. 862–867.
- [31] O. Martinez-Manzanera, E. Roosma, M. Beudel, R. W. K. Borgemeester, T. van Laar, and N. M. Maurits, "A method for automatic and objective scoring of bradykinesia using orientation sensors and classification algorithms," *IEEE Trans. Biomed. Eng.*, vol. 63, no. 5, pp. 1016–1024, May 2016, doi: [10.1109/TBME.2015.2480242](https://doi.org/10.1109/TBME.2015.2480242).

- [32] A. Kandori et al., "Quantitative magnetic detection of finger movements in patients with Parkinson's disease," *Neurosci. Res.*, vol. 49, no. 2, pp. 253–260, Jun. 2004, doi: [10.1016/j.neures.2004.03.004](https://doi.org/10.1016/j.neures.2004.03.004).
- [33] K. Niazmand, K. Tonn, A. Kalaras, U. M. Fietzek, J. H. Mehrkens, and T. C. Lueth, "Quantitative evaluation of Parkinson's disease using sensor based smart glove," in *Proc. 24th Int. Symp. Comput.-Based Med. Syst. (CBMS)*, Jun. 2011, pp. 1–8, doi: [10.1109/CBMS.2011.5999113](https://doi.org/10.1109/CBMS.2011.5999113).
- [34] H. Ling, L. A. Massey, A. J. Lees, P. Brown, and B. L. Day, "Hypokinesia without decrement distinguishes progressive supranuclear palsy from Parkinson's disease," *Brain*, vol. 135, no. 4, pp. 1141–1153, Apr. 2012, doi: [10.1093/brain/aws038](https://doi.org/10.1093/brain/aws038).
- [35] M. Djurić-Jovičić et al., "Finger tapping analysis in patients with Parkinson's disease and atypical parkinsonism," *J. Clin. Neurosci.*, vol. 30, pp. 49–55, Aug. 2016, doi: [10.1016/j.jocn.2015.10.053](https://doi.org/10.1016/j.jocn.2015.10.053).
- [36] D. Krizan et al., "Embedding FBG sensors for monitoring vital signs of the human body: Recent progress over the past decade," *APL Photon.*, vol. 9, no. 8, Aug. 2024, Art. no. 081201, doi: [10.1063/5.0226556](https://doi.org/10.1063/5.0226556).
- [37] D. Lo Presti et al., "Fiber Bragg gratings for medical applications and future challenges: A review," *IEEE Access*, vol. 8, pp. 156863–156888, 2020, doi: [10.1109/ACCESS.2020.3019138](https://doi.org/10.1109/ACCESS.2020.3019138).
- [38] A. Kersey et al., "Fiber grating sensors," *J. Lightw. Technol.*, vol. 15, no. 8, pp. 1442–1463, Aug. 15, 1997, doi: [10.1109/50.618377](https://doi.org/10.1109/50.618377).
- [39] H. E. Joe, H. Yun, S. H. Jo, M. B. Jun, and B. K. Min, "A review on optical fiber sensors for environmental monitoring," *Int. J. Precis. Eng. Manuf.-Green Technol.*, vol. 5, no. 1, pp. 173–191, 2018, doi: [10.1007/s40684-018-0017-6](https://doi.org/10.1007/s40684-018-0017-6).
- [40] P. D. Palma, E. D. Vita, A. Iadicicco, and S. Campopiano, "Force sensor based on FBG embedded in silicone rubber," *IEEE Sensors J.*, vol. 23, no. 2, pp. 1172–1178, Jan. 2023, doi: [10.1109/JSEN.2022.3226039](https://doi.org/10.1109/JSEN.2022.3226039).
- [41] P. D. Palma, E. D. Vita, A. Iadicicco, and S. Campopiano, "Silicone embedded FBGs for force sensing," in *Proc. Annu. Meeting Italian Electron. Soc.*, 2023, pp. 160–165, doi: [10.1007/978-3-031-26066-7_25](https://doi.org/10.1007/978-3-031-26066-7_25).
- [42] E. D. Vita, P. D. Palma, V. R. Marrazzo, G. Breglio, A. Iadicicco, and S. Campopiano, "Fiber Bragg grating embedded in soft patch for finger tapping assessment," in *Proc. IEEE Int. Workshop Metrol. Ind. 4.0 IoT (MetroInd4.0&IoT)*, vol. 17, Jun. 2023, pp. 382–387, doi: [10.1109/metroind4.0iot57462.2023.10180163](https://doi.org/10.1109/metroind4.0iot57462.2023.10180163).
- [43] E. D. Vita, S. Campopiano, M. Cuomo, V. R. Marrazzo, G. Breglio, and A. Iadicicco, "Silicone embedding of fiber Bragg gratings for physiological sensing," in *Proc. 4th URSI Atlantic RadioSci. Conf. (AT-RASC)*, Ghent, Belgium: URSI-International Union Radio Science, 2024, pp. 1–4, doi: [10.46620/ursiatrasc24/bput7357](https://doi.org/10.46620/ursiatrasc24/bput7357).



Elena De Vita (Member, IEEE) received the M.Sc. degree (cum laude) in biomedical engineering from Università Campus Bio-Medico di Roma, Rome, Italy, in 2018, and the Ph.D. degree in information and communication technology and engineering from the University of Naples "Parthenope," Naples, Italy, in 2022.

She is currently a Researcher with the Department of Engineering, University of Naples "Parthenope." Her research focuses on the design, development, and testing of fiber optic sensors for biomedical applications and structural health monitoring.



Vincenzo Romano Marrazzo received the B.Sc. and M.Sc. degrees in electronics engineering and the Ph.D. degree in information technology and electrical engineering from the University of Naples Federico II, Naples, Italy, in 2014, 2017, and 2021, respectively.

He is currently a Researcher with the Department of Electrical Engineering and Information Technology, University of Naples Federico II. His research focuses on the development of fiber optic sensor-based monitoring systems for

various environments, as well as the design and characterization of electronic and optoelectronic systems for sensor reading in both normal and harsh conditions.

Dr. Marrazzo is a member of CMS collaboration at the European Organization for Nuclear Research (CERN) (CH).



Giovanni Breglio received the (cum laude) degree in electronic engineering from the University of Naples Federico II, Naples, Italy, in 1990, and the Ph.D. degree in electronic engineering and computer science from the University of Naples Federico II, in 1994.

He is a Full Professor of Electronics at the University of Naples Federico II. He is a Coordinator with the OptoPower Laboratory, DIETI Department. He has authored more than 90 peer-reviewed journal articles and about 170 proceedings of international conferences. His research interests include the electrothermal modeling and characterization of semiconductor devices for the enhancements of performance design; the development and design of new fiber optical sensors and monitoring systems; and the design of silicon-based optoelectronic devices.

Dr. Breglio is a member of CMS Collaboration at CERN (CH), for the UNINA-DIET@CMS as the Team Leader. In 2023 he has been the Co-General Chair and a TCP Member of the international conference ICSCRM'23, held in Sorrento with more than 1300 attendees worldwide. He is Trach-Chair of the TCP of ESREF'24 International Conference.



Agostino Iadicicco (Member, IEEE) received the (hons.) degree in electronic engineering from the Second University of Naples, Naples, Italy, in 2002, and the Ph.D. degree in information engineering from the Department of Engineering, University of Sannio, Benevento, Italy, in 2005.

In 2006 he joined the Università di Naples "Parthenope," Naples, as an Assistant Professor, where he is presently a Full Professor. He is currently a Coordinator of the Ph.D. Program in "Information and Communication Technology and Engineering."

Since 2002, his research activity has been focused on optoelectronics and photonics devices for sensing and communications applications. He is currently involved in the design, realization, and testing of novel in-fiber devices in standard and unconventional fibers including polarization maintaining and photonic bandgap fibers. His work in this area encompasses the development and practical application of sensors for the measurement of a range of physical, chemical, and biological parameters.

Dr. Iadicicco serves as an Associate Editor for the IEEE Sensors Journal and has been a tutor of several Ph.D. students.



Stefania Campopiano (Member, IEEE) received the master's (cum laude) degree in electronic engineering from the University of Naples Federico II, Naples, Italy, in 1999, and the Ph.D. degree in electronic engineering from the Università della Campania L. Vanvitelli, Caserta, Italy, in 2002.

She is a Full Professor of Electronics and Optoelectronics with the University of Naples "Parthenope," Naples. She is the author of over 200 printed works, including international journals and conferences, co-author of patents, and reviewer for several journals. Her research interests include the development of novel fiber optic sensors for the measurement of physical, chemical, and biological parameters.

Dr. Campopiano is the Chair of the IEEE Sensors Council Italy Chapter.